Atmos. Chem. Phys., 14, 6159–6176, 2014
www.atmos-chem-phys.net/14/6159/2014/
doi:10.5194/acp-14-6159-2014

Atmospheric Chemistry and Physics Open Access

Organic aerosol components derived from 25 AMS data sets across Europe using a consistent ME-2 based source apportionment approach

M. Crippa[1,*], F. Canonaco[1], V. A. Lanz[1], M. Äijälä[2], J. D. Allan[3,17], S. Carbone[4], G. Capes[3], D. Ceburnis[13], M. Dall'Osto[5], D. A. Day[6], P. F. DeCarlo[1,], M. Ehn[2], A. Eriksson[7], E. Freney[8], L. Hildebrandt Ruiz[9,***], R. Hillamo[4], J. L. Jimenez[6], H. Junninen[2], A. Kiendler-Scharr[10], A.-M. Kortelainen[11], M. Kulmala[2], A. Laaksonen[11], A. A. Mensah[10,****], C. Mohr[1,*****], E. Nemitz[12], C. O'Dowd[13], J. Ovadnevaite[13], S. N. Pandis[14], T. Petäjä[2], L. Poulain[15], S. Saarikoski[4], K. Sellegri[8], E. Swietlicki[7], P. Tiitta[11], D. R. Worsnop[2,4,11,16], U. Baltensperger[1], and A. S. H. Prévôt[1]**

[1]Laboratory of Atmospheric Chemistry, Paul Scherrer Institute, 5232 PSI Villigen, Switzerland
[2]Department of Physics, P.O. Box 64, University of Helsinki, 00014 Helsinki, Finland
[3]School of Earth, Atmospheric & Environmental Sciences, The University of Manchester, Manchester, UK
[4]Air Quality Research, Finnish Meteorological Institute, P.O. Box 503, 00101 Helsinki, Finland
[5]Institute of Environmental Assessment and Water Research (IDAEA), CSIC, 08034 Barcelona, Spain
[6]Cooperative Institute for Research in Environmental Sciences (CIRES), Boulder, CO, USA
[7]Division of Nuclear Physics, University of Lund, 221 00 Lund, Sweden
[8]Laboratoire de Météorologie Physique, CNRS-Université Blaise Pascal, UMR6016, 63117, Clermont Ferrand, France
[9]Center for Atmospheric Particle Studies, Carnegie Mellon University, 5000 Forbes Ave., Pittsburgh, PA, 15213, USA
[10]Institut für Energie- und Klimaforschung: Troposphäre (IEK 8), Forschungszentrum Jülich GmbH, Jülich, Germany
[11]Department of Environmental Science, Univ. of Eastern Finland, P.O. Box 1627, 70211 Kuopio, Finland
[12]Centre for Ecology and Hydrology, Bush Estate, Penicuik, Midlothian, EH26 0QB, UK
[13]School of Physics & Centre for Climate & Air Pollution Studies, National University of Ireland Galway, Galway, Ireland
[14]Institute of Chemical Engineering Sciences (ICE-HT), Foundation for Research and Technology Hellas (FORTH), Patras, 26504, Greece
[15]Leibniz Institute for Tropospheric Research, Permoserstr. 15, 04318 Leipzig, Germany
[16]Aerodyne Research, Inc. Billerica, MA, USA
[17]National Centre for Atmospheric Science, The University of Manchester, Manchester, UK
[*]now at: European Commission, Joint Research Centre, Institute for Environment and Sustainability, Air and Climate Unit, Via Fermi, 2749, 21027 Ispra, Italy
[**]now at: Department of Civil, Architectural, and Environmental Engineering and Department of Chemistry, Drexel University, Philadelphia, PA, 19104, USA
[***]now at: The University of Texas at Austin, McKetta Department of Chemical Engineering, Austin, TX, 78712, USA
[****]now at: ETH Zurich, Institute for Atmospheric and Climate Science, Zurich, Switzerland
[*****]now at: Department of Atmospheric Sciences, University of Washington, Seattle WA 98195, USA

Correspondence to: A. S. H. Prévôt (andre.prevot@psi.ch)

Received: 7 August 2013 – Published in Atmos. Chem. Phys. Discuss.: 5 September 2013
Revised: 18 April 2014 – Accepted: 3 May 2014 – Published: 23 June 2014

Published by Copernicus Publications on behalf of the European Geosciences Union.

Abstract. Organic aerosols (OA) represent one of the major constituents of submicron particulate matter (PM_1) and comprise a huge variety of compounds emitted by different sources. Three intensive measurement field campaigns to investigate the aerosol chemical composition all over Europe were carried out within the framework of the European Integrated Project on Aerosol Cloud Climate and Air Quality Interactions (EUCAARI) and the intensive campaigns of European Monitoring and Evaluation Programme (EMEP) during 2008 (May–June and September–October) and 2009 (February–March). In this paper we focus on the identification of the main organic aerosol sources and we define a standardized methodology to perform source apportionment using positive matrix factorization (PMF) with the multilinear engine (ME-2) on Aerodyne aerosol mass spectrometer (AMS) data. Our source apportionment procedure is tested and applied on 25 data sets accounting for two urban, several rural and remote and two high altitude sites; therefore it is likely suitable for the treatment of AMS-related ambient data sets. For most of the sites, four organic components are retrieved, improving significantly previous source apportionment results where only a separation in primary and secondary OA sources was possible. Generally, our solutions include two primary OA sources, i.e. hydrocarbon-like OA (HOA) and biomass burning OA (BBOA) and two secondary OA components, i.e. semi-volatile oxygenated OA (SV-OOA) and low-volatility oxygenated OA (LV-OOA). For specific sites cooking-related (COA) and marine-related sources (MSA) are also separated. Finally, our work provides a large overview of organic aerosol sources in Europe and an interesting set of highly time resolved data for modeling purposes.

1 Introduction

Atmospheric aerosols negatively affect human health (Pope and Dockery, 2006), reduce visibility, and interact with climate and ecosystems (IPCC, 2007). Among particulate pollutants, great interest is dedicated to organic aerosols (OA) since they can represent from 20 to 90 % of the total submicron mass (Zhang et al., 2007; Jimenez et al., 2009). Organic aerosols are ubiquitous and are directly emitted by various sources, including traffic, combustion activities, biogenic emissions, and can also be produced via secondary formation pathways in the atmosphere (Hallquist et al., 2009). Constraining OA emission sources and understanding their evolution and fate in the atmosphere is therefore fundamental to define mitigation strategies for air quality.

Our work is part of the European Integrated Project on Aerosol Cloud Climate and Air Quality Interactions (EUCAARI), which aims to understand the interactions between air pollution and climate. An introduction about project objectives and an overview on the goals reached within the EUCAARI project are provided by several papers (Kulmala et al., 2009, 2011; Knote et al., 2011; Fountoukis et al., 2011; Murphy et al., 2012). The coordinated EUCAARI campaigns of 2008 and 2009 provide significantly more aerosol mass spectrometer (AMS) data sets to analyze in comparison to previous efforts (Aas et al., 2012). For the investigation of the aerosol chemical composition and organic aerosol (OA) sources dedicated studies were performed. Nemitz et al. (2014) discuss the organic and inorganic components of atmospheric aerosols, using AMS measurements performed during three intensive field campaigns in 2008 and 2009. Major contribution to the submicron particulate matter (PM_1) mass is provided by the organic compounds, which contribute from 20 to 63 % to the total mass depending on the site. Our work deals with the identification and quantification of organic aerosol sources in Europe using high time resolution data from aerosol mass spectrometer. Here we focus on the investigation of OA sources applying the positive matrix factorization algorithm (PMF) running on the generalized multi-linear engine (ME-2) (Paatero, 1999; Canonaco et al., 2013) to the organic AMS mass spectra from all over Europe.

Currently, only a few studies concerning a broad spatial overview of OA sources are available in the literature. Zhang et al. (2007) investigated organic aerosol sources in urban and anthropogenically influenced remote sites in the Northern Hemisphere, focusing on the discrimination between the traffic-related and secondary oxygenated OA components. Jimenez et al. (2009) presented an overview of PM_1 chemical composition all over the world (including 8 European measurement sites) focusing on the identification of OA sources using AMS data. Ng et al. (2010) provided an overview of OA sources in the Northern Hemisphere, including a broader spatial domain than Europe and a wide range of locations affected by different aerosol sources. Moreover, their major focus was the investigation of the secondary oxygenated components and their aging. Lanz et al. (2010) provided an overview of the aerosol chemical composition and OA sources in central Europe focusing on Switzerland, Germany, Austria, France, and Liechtenstein. In all of these studies, the major fraction of PM_1 was often represented by organics which consisted, for most of the locations, of oxygenated OA; however the contribution of primary sources (like traffic and biomass burning) was not always identified especially in rural and remote places. Our work includes 17 measurement sites all over Europe, comprising 25 unit mass resolution AMS data sets, and represents therefore an unprecedented overview of OA sources in Europe. Moreover, the application of advanced source apportionment methods allow us to overcome limitations of commonly used source apportionment techniques for AMS data, such as the purely unconstrained positive matrix factorization (Canonaco et al., 2013). The positive matrix factorization (PMF) model does not always succeed since the co-variance of the sources might be large due to the meteorology and the relative source contributions

which vary too little. This can often be the case at rural and remote sites but it was also shown for an urban background site in Zurich, for which Lanz et al. (2008) pioneered the use of ME-2 for AMS data. Here, for all measurement sites we are able to clearly separate primary and secondary OA components, including hydrocarbon-like OA (HOA, associated with traffic emissions), biomass burning OA (BBOA), cooking (COA) and secondary components (semi-volatile and low volatility oxygenated OA, SV-OOA and LV-OOA, respectively).

In addition, we provide a standardized source apportionment procedure applicable to any measurement site (urban, rural, remote, etc.) guiding source apportionment analysis for on-line measurements. In fact, when applying multivariate methods to AMS data, a critical phase is the evaluation of the results which is strongly affected by subjectivity and obviously depends on the expertise of the researcher. One goal of this work is to facilitate the analysis of the modeler dealing with AMS data; additionally, this strategy might be useful in particular for the analysis of the long-term monitoring network data retrieved with the quadrupole or time-of-flight aerosol chemical speciation monitors (ACSM) (Ng et al., 2011b; Fröhlich et al., 2013)

A final motivation of our work is to improve the prediction of POA (primary organic aerosol) and SOA (secondary organic aerosol) in regional and global models integrating our European overview of OA sources. Our source apportionment results are suitable for modeling purposes since understanding sources and processes of organic aerosols can substantially improve air quality and climate model predictions. Modeling POA and SOA components is challenging and still critical due to uncertainties in emission inventories and complex atmospheric processing. Including measurements of different OA components will improve the evaluation and constraining of modeling outputs. Our results will help in evaluating the accuracy of emission inventories (especially concerning primary sources) which need better constraints to improve regional and global models (Kanakidou et al., 2005; De Gouw and Jimenez, 2009), while SOA sources obtained from AMS source apportionment could be used to constrain SOA in global chemical transport models (Spracklen et al., 2011).

2 Measurement field campaigns

2.1 Overview of the EUCAARI/EMEP 2008-2009 campaigns

Three intensive measurement field campaigns were performed during late Spring 2008 (May–June), Fall 2008 (September–October) and Winter 2009 (February–March) within the European Integrated Project on Aerosol Cloud Climate and Air Quality interactions (EUCAARI) to investigate the chemical composition of atmospheric aerosols in Europe among several other objectives (Kulmala et al., 2009).

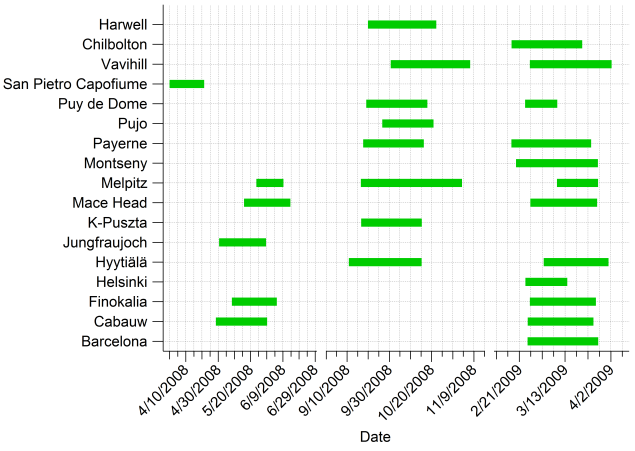

Figure 1. EUCAARI/EMEP campaigns 2008–2009: measurement periods.

Aerosol mass spectrometer (AMS) measurements were carried out during 26 field campaigns at 17 different sites (see Fig. 1), which are classified as urban (UR, including Barcelona and Helsinki), rural (RU, including Cabauw, Payerne, Montseny, San Pietro Capofiume, Melpitz, Puijo, Chilbolton, Harwell, K-Puszta, and Vavihill), remote (RE, including Finokalia, Mace Head, and Hyytiälä) and high altitude (HA, including Jungfraujoch and Puy de Dome) (Nemitz et al., 2014). For some of the sites, specific studies were also published. We refer the reader to Mohr et al. (2012) for the Barcelona 2009 campaign, to Hildebrandt et al. (2010a, b, 2011) for the Finokalia 2008 and 2009 campaigns, to Mensah et al. (2012), Li et al. (2013), and Paglione et al. (2013) for the Cabauw 2008 campaign, to Saarikoski et al. (2012) for the San Pietro Capofiume measurements, to Carbone et al. (2014) for the case of Helsinki, to Poulain et al. (2011) for Melpitz, to Dall'Osto et al. (2010) for Mace Head, and to Freney et al. (2011) for Puy de Dome. An overview about PM_1 aerosol chemical composition is provided in a companion paper by Nemitz et al. (2014), where a detailed discussion about measurements setup and data processing is also provided. The average concentrations of PM_1 chemical components as measured by the AMS are also reported in Table S1 in the Supplement. In this paper we focus on the organic aerosols (OA) component which represents the major fraction of submicron particulate matter for most of the sites, ranging between 20 and 63 % of PM_1 (concentration range: 0.6–8.2 $\mu g\,m^{-3}$), consistent with the values found by Jimenez et al. (2009) and Ng et al. (2010). Table 1 summarizes the average organic concentration for each site and all the seasons and the relative OA contribution to NR-PM_1 as measured by the AMS. Figure 2 represents an overview of the EUCAARI measurement field campaigns focusing on the organic aerosol sources (an analogous plot for the PM_1 chemical composition is reported in Nemitz et al. (2014)). For each site the average organic mass concentration of

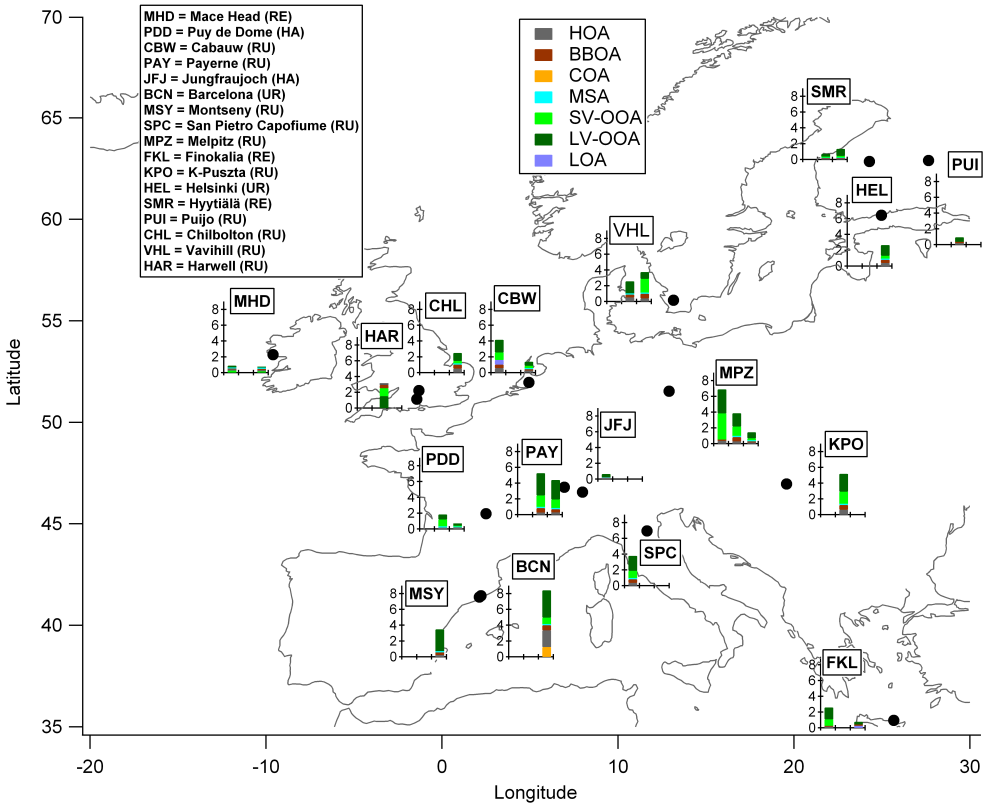

Figure 2. Measurement sites and average organic aerosol source contributions (bars). Measurement sites are classified according to their location as urban (UR), rural (RU), remote (RE) and high altitude (HA). The bar graphs report the average OA source concentrations (y-axis in $\mu g\,m^{-3}$) for the three measurement periods (the chronological order is from left to right: spring 2008, fall 2008 and spring 2009 campaigns, respectively). The identified OA sources are: HOA (hydrocarbon-like OA), BBOA (biomass burning OA), COA (cooking OA), SV-OOA and LV-OOA (semi-volatile and low-volatility oxygenated OA), MSA (methane sulfonic acid) and LOA (local OA).

primary and secondary sources is shown as apportioned by our standard ME-2 approach. Results from the three measurement periods are represented with separated bars following the chronological order from left to right (spring 2008, fall 2008 and spring 2009 campaigns, respectively). Figures S2.1, S2.2, and S2.3 show the time series of the relative contributions of each OA factor for all the measurement sites during the three campaigns. Details about our source apportionment strategy exploiting the multi-linear engine (ME-2) are discussed in Sects. 3 and 4.

2.2 Aerosol mass spectrometer measurements

The Aerodyne aerosol mass spectrometer measures size-resolved mass spectra of the non-refractory (NR) PM_1 aerosol species, where NR species are operationally defined as those that flash vaporize at 600 °C and 10^{-5} Torr. Black carbon, mineral dust, and metals usually cannot be detected and quantified by the AMS, while Ovadnevaite et al. (2012) shown the possibility to measure sea salt with the AMS. Several aerosol mass spectrometers were deployed all over Europe during the three intensive EUCAARI field campaigns

Table 1. Average organic concentrations (OA) and their relative contributions to the NR-PM_1 mass measured by the AMS.

Site	OA ($\mu g\,m^{-3}$)	OA/NR-PM_1
Barcelona	8.20	0.50
Cabauw	2.60	0.31
Finokalia	2.00	0.36
Helsinki	2.90	0.38
Hyytiälä	1.10	0.45
Jungfraujoch	0.66	0.43
K-Puszta	5.30	0.45
Mace Head	0.85	0.39
Melpitz	4.07	0.40
Montseny	3.50	0.32
Payerne	4.75	0.42
Puijo	0.90	0.64
Puy de Dome	1.17	0.28
San Pietro Capofiume	3.80	0.39
Vavihill	3.15	0.39
Chilbolton	2.50	0.28
Harwell	3.21	0.33

(Nemitz et al., 2014), including Q-AMS (quadrupole AMS) (Jayne et al., 2000), C-ToF-AMS (compact time of flight AMS) (Drewnick et al., 2005) and HR-ToF-AMS (high resolution time of flight AMS) (DeCarlo et al., 2006).

The general working principle of the AMS is reported below; however the reader should refer to the aforementioned papers for a detailed description of the different AMS types. Briefly, air is sampled through a critical orifice into an aerodynamic lens, where the aerosol particles are focused into a narrow beam and accelerated to a velocity inversely related to their aerodynamic size. Particles are transmitted into a high vacuum detection chamber (10^{-5} Torr) and impact on a heated surface (600 °C) where the non-refractory species vaporize. The resulting gas molecules are ionized by electron impact (EI, 70 eV) and the ions are extracted into the detection region to be classified by the mass spectrometer. Details about our AMS measurement quantification and data treatment (e.g., ionization efficiency calibrations, collection efficiency estimation, air corrections, etc.) are described elsewhere (Nemitz et al., 2014). For the evaluation of our source apportionment results, black carbon data obtained from aerosol light absorption measurements performed with an aethalometer or a multi angle absorption photometer (MAAP) were also used in our work where available (see Table S3).

3 Organic aerosol source apportionment

3.1 The multilinear engine (ME-2)

Positive matrix factorization (PMF) is the most commonly used source apportionment method for AMS data (Lanz et al., 2007; Ulbrich et al., 2009; Zhang et al., 2011) to describe the measurements with a bilinear factor model (Paatero and Tapper, 1994):

$$\mathbf{x}_{ij} = \sum_{k=1}^{p} \mathbf{g}_{ik} * \mathbf{f}_{kj} + \mathbf{e}_{ij} \quad (1)$$

where x_{ij}, g_{ik}, f_{kj} and e_{ij} represent the matrix elements of the measurements (**x**), time series (**g**), factor profiles (**f**), and residuals (**e**). The subscript i corresponds to time, j to m/z, k to a discrete factor and p to the number of factors. The model solution is found iteratively minimizing Q using the least squares algorithm:

$$Q = \sum_{i=1}^{m} \sum_{j=1}^{n} \left(\frac{e_{ij}}{\sigma_{ij}} \right)^2, \quad (2)$$

where σ_{ij} are the measurement uncertainties.

The model solution is not unique due to rotational ambiguity (Paatero et al., 2002), in fact the product of the rotated matrix $\overline{\mathbf{G}}$ and $\overline{\mathbf{F}}$ ($\overline{\mathbf{G}} = G \cdot T$ and $\overline{\mathbf{F}} = T^{-1} \cdot F$) is equal to the product of the corresponding unrotated matrix which also provides the same value of the object function Q. In order to reduce rotational ambiguity within the ME-2 algorithm, the user can add a priori information into the model (e.g., source profiles), so that it does not rotate and it provides a rather unique solution (Paatero and Hopke, 2009).

We perform organic aerosol source apportionment using the multi-linear engine (ME-2) algorithm (Paatero, 1999) implemented within the toolkit SoFi (Source Finder) developed by Canonaco et al. (2013) at Paul Scherrer Institute. Similarly to the PMF solver (Paatero and Tapper, 1994), the ME-2 solver (Paatero, 1999) executes the positive matrix factorization algorithm. However, the user has the advantage to support the analysis by introducing a priori information in form of known factor time series and / or factor profiles, for example within the so-called a value approach (see Eqs. (3a) and (3b)). The a value (ranging from 0 up to values larger than 1) determines how much the resolved factors ($f_{j,\text{solution}}$) and $g_{i,\text{solution}}$) are allowed to vary from the input ones (f_j, g_i), as defined in Eq. (3a) and (3b) (Canonaco et al., 2013). In our work we only constrained the mass spectra represented by f.

$$f_{j,\text{solution}} = f_j \pm \alpha \cdot f_j \quad (3a)$$

$$g_{i,\text{solution}} = g_i \pm \alpha \cdot g_i \quad (3b)$$

For example, if $a = 0.1$ when constraining a mass spectral profile, all of the m/z's in the fit profile can vary as much as −10 % to +10 % of the input constraining mass spectrum profile.

In our work, a constant a value is applied to the entire constrained mass spectra (MS); however a softer constraining technique is provided by the pulling approach (Paatero and Hopke, 2009; Brown et al., 2012), which is available within the SoFi package (Canonaco et al., 2013) and which is explained in more detail in Canonaco et al. (2014b).

The ME-2 solver is here successfully applied to the time series of the unit mass resolution organic mass spectra measured by the AMS, including for most of the sites m/z up to 200 (for a few sites the analysis was performed only up to m/z 150 due to the low signal to noise ratio (SNR) observed). Data are first averaged to 15–30 minute time resolution and after performing the source apportionment analysis they are averaged to 1 hour for modeling purposes. The error matrix preparation before running the source apportionment algorithm is performed following the procedure introduced by Ulbrich et al. (2009). Briefly, a minimum counting error of 1 ion is applied, m/z with SNR between 2 and 0.2 (weak variables) are downweighted by a factor of 2, while bad variables (SNR<0.2) are downweighted by a factor of 10 (Paatero and Hopke, 2003; Ulbrich et al., 2009). Moreover, based on the AMS fragmentation table, some organic masses are not directly measured but calculated as a fraction of the organic signal at m/z 44 (Allan et al., 2004); therefore the errors of these m/z 44 dependent peaks are downweighted (Ulbrich et al., 2009).

3.2 A standardized source apportionment strategy

In this section we provide technical guidelines to perform a standard source apportionment analysis on AMS data in order to identify well known organic aerosol sources, like hydrocarbon-like (HOA), biomass burning (BBOA), cooking (COA) and oxygenated components (OOA), but also site-specific sources. Our approach is particularly relevant for rural locations where the temporal variability of emission sources is less distinct and where the aging processes are dominant compared to fresh emissions. A detailed description of the main features of these OA sources (source profile, diurnal patterns, etc.) is presented in Sect. 4. Here, we define first our source apportionment strategy and then we provide details about the application of this methodology on the EUCAARI-EMEP data. Finally, some technical examples concerning the data treatment and interpretation are also reported in Sects. 3.2.2 and 3.2.3.

3.2.1 Technical guidelines

Within our work we define a standardized methodology to perform source apportionment on AMS data using the ME-2 algorithm with the aforementioned SoFi toolkit (Paatero, 1999; Canonaco et al., 2013). The sequential steps of the methodology are reported below:

1. Unconstrained run (PMF).
2. Constrain the HOA mass spectrum (MS) with a low a value (e.g., a =0.05–0.1) and test various number of factors.
3. Look for BBOA (if not identified yet): constrain the BBOA MS if f_{60} (i.e., the fraction of m/z 60 to the total organic mass) is above background level and check temporal structures like diurnal increases in the evening during the cold season due to domestic wood burning (suggested a value = 0.3–0.5).
4. Look for COA (if cooking not found yet): check the f_{55}–f_{57} plot for cooking evidence (where f_{55} and f_{57} are the fraction of m/z 55 and m/z 57 to the total organic mass respectively; see Mohr et al., 2012). Fix it in any case and check its diurnal pattern (the presence of the meal hour peaks is necessary to support it at least in urban areas).
5. Residual analysis: a structure in the residual diurnals might indicate possible sources not separated yet by the model (refer to Section 3.2.3). For each step the residual plots should always be consulted in order to evaluate whether the constrained profile(s) has(have) caused structures in the residuals. If so, the constrained profile should be tested with a higher scalar a value.
6. In general the OOA components are not fixed, but are left as 1 to 3 additional unconstrained factors.

Our approach starts with an unconstrained run, where no a priori information concerning the source mass spectra is added. This first step is important because it reveals the possibility of separation for several OA components with PMF. It also gives the user an idea of the number of possible sources for that site, even though they might not be clearly separated yet. If the HOA mass spectrum is not identified in the first step (e.g., considering from 1 to 5 unconstrained factors), the user should fix the HOA mass spectrum with the a value approach and, to evaluate the presence of this source into the data set, investigate its diurnal pattern and correlation with available external tracers (e.g., black carbon, NOx, etc.). At this step several constrained runs are required varying the number of unconstrained factors (e.g., from 3 to 5) in order to investigate the presence of other possible sources (e.g., BBOA, COA, secondary components and possibly specific site-related factors). Moreover, the user should perform a sensitivity analysis on the a value associated with the HOA MS in order to define a range of possible solutions. A detailed discussion about the sensitivity analysis is reported in Sect. 4.5. If the user is unable to identify a biomass burning related source within step 2, the investigation of the diurnal pattern of a specific organic tracer for levoglucosan and primary biomass combustion species ($f_{60} = m/z$ 60 / OA) (Alfarra et al., 2007) can reveal the presence of BBOA at the site (e.g., increasing contribution of f_{60} during the evening suggests the use of biomass burning for domestic heating purposes). In addition, it is important to study the variability of f_{60} above background levels, which is reported to be 0.3 % ± 0.06 % (DeCarlo et al., 2008; Aiken et al., 2009; Cubison et al., 2011). Finally, a primary OA source especially important in urban areas is cooking (COA) (Slowik et al., 2010; Allan et al., 2010; Sun et al., 2011; Mohr et al., 2012; Crippa et al., 2013). The cooking contribution is not easily resolved even for urban sites due to the similarity of its mass spectrum with the one of HOA in unit mass resolution. So after identifying HOA and BBOA, the user should constrain the COA MS with a rather low a value (e.g., a =0.05). To interpret the retrieved factor as a cooking-related source, its diurnal pattern should show two peaks corresponding to the meal hours at least in urban or semi-urban sites. As demonstrated in Fig. 6 of Mohr et al. (2012), the f_{55} vs. f_{57} plot can provide further evidence of COA in urban sites strongly affected by cooking activities. In fact, the triangular space defined by Mohr et al. (2012) allows the identification of cooking-influenced OA for points lying on the left hand side of this triangle which are dominated by f_{55} (and therefore cooking emissions) compared to points dominated by the traffic source (lying on the right hand side of the triangle).

For specific sites (e.g., coastal locations, etc.) different sources from continental urban and rural locations can be expected. Therefore any a priori knowledge about specific OA sources should be constrained when running the ME-2 engine, to drive the model in finding local sources, often characterized by low contribution in mass and reduced

temporal variability. Technical examples are provided in Sect. 3.2.2.

At each step of the discussed methodology, it is important to evaluate how the residuals vary moving from one step to the other, and within a single phase varying the number of factors. After fixing HOA and BBOA (step 3), the investigation of the average diurnal variation of the residuals can highlight the presence of unresolved sources by the model (refer to Sect. 2.3.3 for further discussion).

When using the ME-2 algorithm for fixing source profiles, the user must carefully validate the obtained results since a good solution is not selected based on the possibility to retrieve a constrained profile (which is expected as output of the model), but on several concurrent validation procedures. The toolkit SoFi created by Canonaco et al. (2013) greatly helps in performing all the suggested steps of our source apportionment methodology and provides several metrics to evaluate the quality of the chosen solution (e.g., correlation with external data time series and mass spectra, detailed residuals analysis, explained/unexplained variation plots etc.) and also an efficient comparison of different solutions (see SoFi manual, http://www.psi.ch/acsm-stations/me-2).

3.2.2 Application to the EUCAARI-EMEP data

The previously mentioned procedure is successfully applied on the 25 available organic AMS data sets and therefore it provides a consistent methodology. Deploying the ME-2 solver allows the discrimination of traffic and biomass burning within the primary sources and of two OOA components for the secondary fraction for most of the sites. In order to perform a value runs within the ME-2 solver, it is necessary to select reference mass spectra to be constrained in the model. Due to the similar features of the HOA and COA mass spectra, in our work we choose the HOA and COA mass spectra identified in Paris by Crippa et al. (2013) as a reference, because of the significant contribution of the cooking source to the total OA mass and its strong diurnal pattern at that site. Solutions from other sites may have cooking and HOA mixed to some extent. For the BBOA reference mass spectrum we adopt the one introduced by Ng et al. (2011a) since it is considered representative of averaged ambient biomass burning conditions. A detailed sensitivity analysis investigating the impact of the input MS on the final solution is already ongoing and will be fully addressed in Canonaco et al. (2014a).

Additionally, for the two marine measurement sites (Mace Head and Finokalia), a methane sulfonic acid (MSA) factor is used too (see Sect. S5). First, a relatively clean MSA MS is obtained through an unconstrained PMF run for the Mace Head 2008 late spring campaign (see Fig. S5 of the supplementary material), during which high biological activity is expected (Dall'Osto et al., 2010). As a second step, this MSA MS is used as input to the algorithm for the two other field campaigns (Finokalia 2008 and Mace Head 2009). The separation of this factor is a challenge for the unconstrained PMF, due to reduced biological activity during early spring in Mace Head and weak marine influence for the site in Crete. Finally, in order to provide a complete overview of the EUCAARI 2008–2009 data, the PMF solution described in this paper for the Finokalia 2009 campaign is reported in this work. Our standardized procedure could not be applied to this data set due to specifics of the data pre-treatment and the presence of unusual local sources.

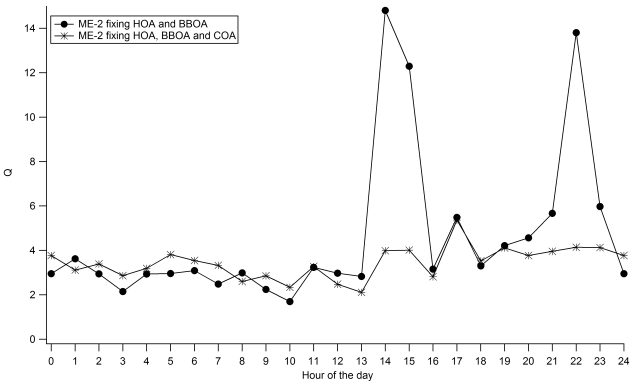

Figure 3. Comparison of the diurnal pattern of the Q-value for the 5-factor solution constraining HOA-BBOA or HOA-BBOA-COA (Barcelona 2009). The structure in the scaled residuals suggests the presence of additional sources.

3.2.3 Technical example of structure in the residuals

As discussed in Sect. 3.2.1, the analysis of the residual structure is fundamental to understand how the model solution varies when adding more factors and which variables and/or events get more explained. Figure 3 shows how the average diurnal profile of the scaled residuals (Q) for Barcelona changes for the 5-factor solution run when constraining HOA and BBOA and when additionally constraining COA. In the first case, the Q diurnal shows two prominent peaks corresponding to the meal hours in Barcelona (Mohr et al., 2012), which suggests the presence of a possible cooking source not resolved yet by the model. Therefore the residual analysis provides an additional good reason to use the ME-2 algorithm to also constrain a cooking source. After constraining the COA mass spectrum in the model, the performance of the model improves since the structure observed in the diurnal profile of the residuals disappears.

4 Results and discussion

4.1 Primary and secondary OA source contributions

The standardized source apportionment strategy introduced in Sect. 3.2 is systematically applied to the 25 available

Table 2. Relative contributions of the identified organic components to the total OA. Note that only main organic sources in common for most of the sites are reported (HOA, BBOA, SV-OOA and LV-OOA).

Site	Spring 2008				Fall 2008				Spring 2009			
	HOA	BBOA	SV-OOA	LV-OOA	HOA	BBOA	SV-OOA	LV-OOA	HOA	BBOA	SV-OOA	LV-OOA
Barcelona									0.24	0.08	0.20	0.29
Cabauw	0.14	0.10	0.22	0.39					0.19	0.10	0.34	0.36
Finokalia	0.04	–	0.33	0.58								0.66
Helsinki									0.16	0.14	0.20	0.51
Hyytiälä					0.06	0.04	0.42	0.48	0.03	0.05	0.28	0.65
Jungfraujoch	0.06	0.11	–	0.83								
K-Puszta					0.12	0.11	0.33	0.44				
Mace Head	0.12	0.16	0.28	0.39					0.12	0.27		0.59
Melpitz	0.05	–	0.51	0.44	0.08	0.14	0.35	0.43	0.09	0.11	0.28	0.52
Montseny									0.07	0.09	–	0.83
Payerne					0.06	0.12	0.28	0.53	0.07	0.09	0.27	0.57
Puijo					0.22	–	–	0.78				
Puy de Dome					0.01	0.09	0.55	0.35	0.06	0.18	0.37	0.39
San Pietro Capofiume	0.10	0.12	0.28	0.50								
Vavihill					0.20	0.12	–	0.68	0.21	0.10	0.50	0.19
Chilbolton									0.20	0.20	0.19	0.40
Harwell					0.07	0.13	0.32	0.48				

AMS data sets, consisting of the AMS matrices with the organic mass spectra over time and the corresponding errors. Table S2 reports the comparison of the number of OA components identified with the a value approach in comparison with the unconstrained run (PMF) (Ulbrich et al., 2009), highlighting in red the constrained source mass spectra. The unconstrained PMF often cannot provide a clear separation of OA sources in rural and remote sites (Zhang et al., 2007; Jimenez et al., 2009). This may also happen at urban background sites where the effect of meteorology can still be dominant compared to the source temporal variability (Lanz et al., 2008; Canonaco et al., 2013). In our 25 data sets, unconstrained PMF allows mainly the identification of POA (often including HOA and BBOA in one factor typically characterized by high signal at m/z 44 and 60) and SOA sources (refer to Table S2). Even when HOA is identified, it is often not clean due to the high contribution of m/z 44 (which should be rather small for primary traffic emissions). In some cases it is only possible to separate two secondary oxygenated components, but no primary source is retrieved, although expected.

On the contrary, with our approach, primary and secondary OA sources are retrieved for all the analyzed data sets, including traffic (HOA), cooking (COA) and biomass burning (BBOA) as primary sources, and methane sulfonic acid (MSA), semi-volatile and low-volatility oxygenated OA (SV-OOA and LV-OOA) as secondary components. For the Cabauw 2008 and Finokalia 2009 data sets the contribution of local (site specific) sources is also observed. The ME-2 solution for the Cabauw 2008 campaign includes a site specific factor (named here LOA, local organic aerosol) which is interpreted to be hulis-related (humic-like substances), as widely explained in Paglione et al. (2013). These results represent a great improvement in the source apportionment field, since we demonstrate the possibility to identify several primary and secondary OA components even at rural locations where the POA factors often contribute less than 10 % of the OA. Comparisons with previously published PMF solutions (mainly from HR-PMF data) for specific sites are reported in Sect. S3 of the supplementary material.

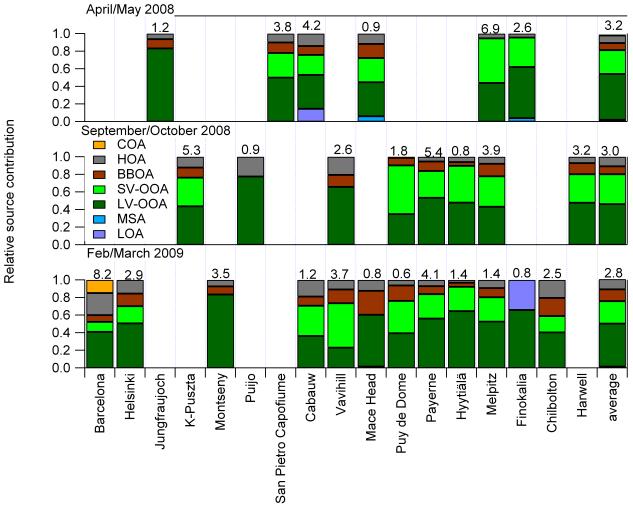

Figure 4. Relative organic source contributions (ME-2 results). On top of each bar the average organic concentration (in $\mu g\,m^{-3}$) is also reported. Site specific sources are classified as LOA (local organic aerosols) and include HULIS-related OA (humic-like substances) for Cabauw (Paglione et al., 2013), while amines and local sources for Finokalia (Hildebrandt et al., 2011).

Our methodology combines the advantages of the chemical mass balance and the positive matrix factorization approach. In fact, the a priori knowledge of well-known source profiles (e.g., from primary sources) drives the source apportionment algorithm in finding an optimal solution for the

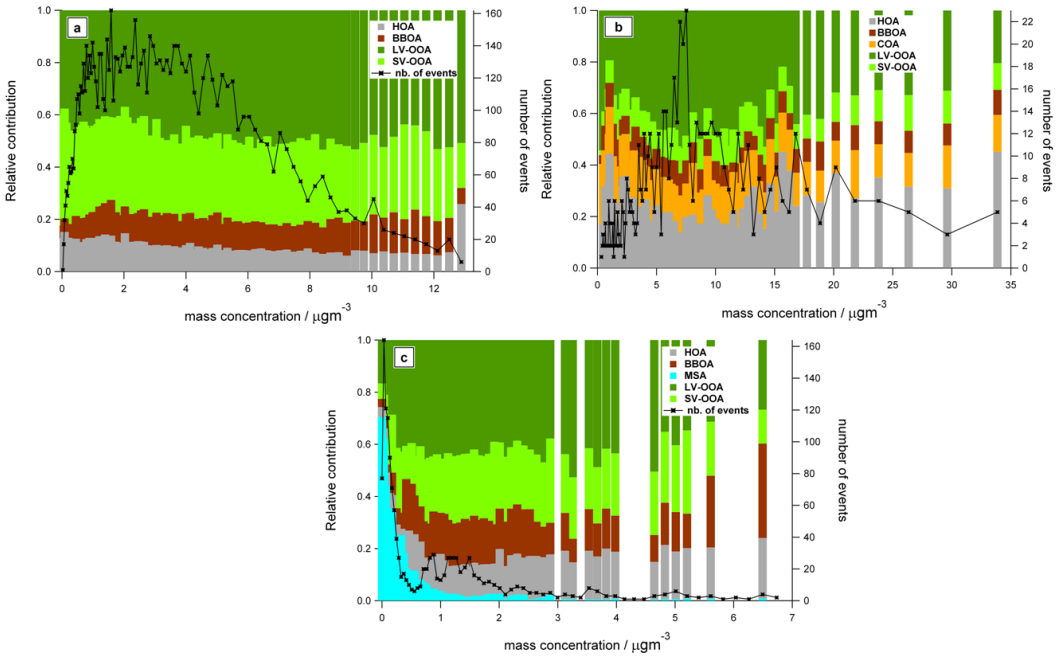

Figure 5. Relative organic source contributions as a function of total organic concentrations. Average plot over all the seasons and rural sites **(a)**, Barcelona only **(b)**, and average plot for marine sites **(c)**.

model, while less constrained components (e.g., secondary OA) are allowed to freely vary (similarly to the unconstrained PMF case). However, our approach should provide consistent results with the unconstrained PMF case, where an optimal solution could be also identified by the means of other techniques such as e.g., a significant number of seeds, individual rotations or by reweighting specific uncertainties, etc., although requiring often very high time efforts and a lot of expertise on the user side.

Figure 4 summarizes the average organic aerosol concentration and the average relative contribution of each OA source for each site (see also Table 2). For all sites and campaigns it is possible to separate a hydrocarbon-like OA factor (average equal to 11 ± 6 % of OA), whose contribution on average ranges from 3 % to 24 % to the total OA mass. The HOA average concentration ranges between 0.1 and 2.1 µg m^{-3} depending on the site location and campaign. Although Puijo is classified as rural site, it has nearly the largest HOA fraction since located on a hill at 2 km from the city center of Kuopio (population 97000) which is a source of HOA and few point sources (Leskinen et al., 2012; Hao et al., 2013). However, in absolute terms, HOA concentrations in Puijo are rather low (0.2 µg m^{-3}), while at sites with high total OA concentrations the absolute HOA amount is higher compared to rural sites.

Biomass burning is identified in 22 data sets and is associated with a mix of domestic heating during cold periods and open fires (e.g., agricultural, forest and gardening waste) and barbecuing activities etc. The BBOA contribution to the total OA mass varies on average between 5 and 27 % (corresponding to 0.1–0.8 µg m^{-3}) with an average relative contribution to the total OA mass equal to 12 ± 5 %. At 3 sites (Melpitz spring 2008, Puijo fall 2008 and Finokalia spring 2008) f_{60} is close to or below the background values and the BBOA is regarded as negligible. Major contribution to total OA derives from secondary sources, which are classified here based on their degree of oxygenation as SV-OOA and LV-OOA and which contribute on average 34 ± 11 % and 50 ± 16 % to the total OA mass, respectively.

Cooking contributes on average ∼15 % to the total OA mass in Barcelona, consistent with AMS ambient measurements performed in European urban areas like Zurich, Paris, London, etc. (Mohr et al., 2012; Canonaco et al., 2013; Crippa et al., 2013; Allan et al., 2010). Finally, MSA contributes from 2 % to 6 % to the total OA mass in the two marine sites (Mace Head and Finokalia), similarly to the values reported by Dall'Osto et al. (2010) and Ovadnevaite et al. (2014).

Figure 5 is an alternative method to summarize source apportionment results, in fact instead of reporting average concentrations of the sources, it reports the relative OA source contribution vs. the OA concentration for all the rural, marine and urban sites, highlighting the role of specific sources within different concentration ranges (average over 21, 1 and 3 data sets for panel a, b and c, respectively). The number of measurements happening for each concentration bin is reported (black line with markers) and shows a decreasing

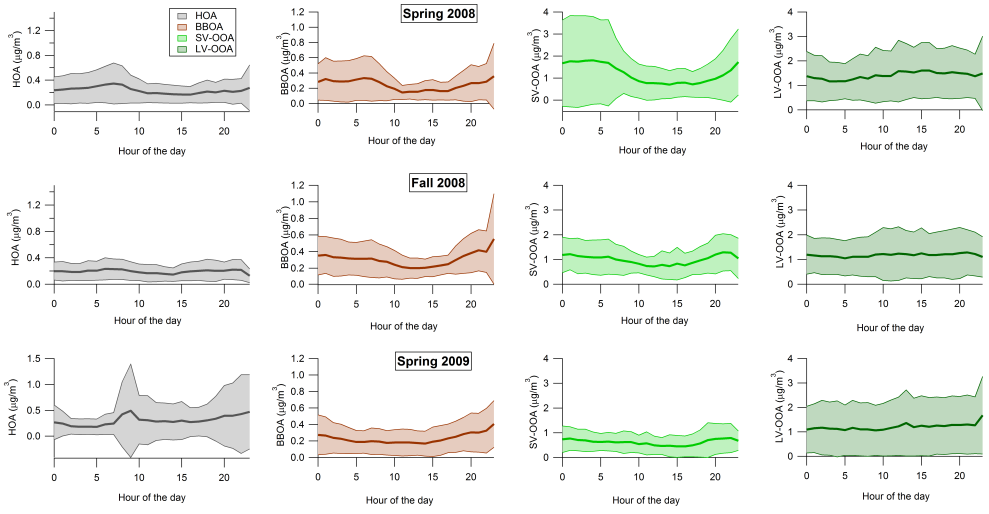

Figure 6. Diurnal profiles of organic aerosol components. Mean values (± standard deviation) for OA components are shown for the different seasons and all sites.

trend for higher concentration. The last concentration bin includes all data points above that concentration.

For rural sites (see Fig. 5a), the HOA contribution decreases with increasing OA concentrations, while the BBOA contribution is very small for very low concentrations (<1 $\mu g\,m^{-3}$), but stable over the rest of the concentration range. No general pattern can be observed for the two secondary components. However the LV-OOA fraction seems to increase at higher concentration. For an urban site like Barcelona (see Fig. 5b), traffic is a significant source both at low and high OA concentrations, while the semi-volatile oxygenated component is rather low. However, the differentiation between SV- and LV-OOA is highly dependent on the oxidation processes in the atmosphere, geographical position of the measurement site, season, meteorological conditions, etc., therefore our conclusions for the Barcelona site might not have general validity. Figure 5c shows the fractional contribution of OA sources as a function of total OA concentration for marine sites. An interesting feature is the high relative contribution of MSA at very low OA concentrations (below 1 $\mu g\,m^{-3}$), where both the primary OA sources and the LV-OOA fraction are small. Figure 5 highlights the importance of comparing models and measurements in different concentration ranges instead of only e.g., the average contributions. An obvious example is Mace Head where the contribution of sources at low concentrations from the Atlantic are very different from situations when the station is downwind of European pollution.

4.2 Evaluation of results

The interpretation of the retrieved source apportionment factors as organic aerosol sources is based on correlations with external data (see Table S3), the investigation of their diurnal pattern (Fig. 5) and the source mass spectra comparison with reference ones (refer to Sect. 4.3 for further discussion). However, presenting all details about the evaluation of the source apportionment results for each campaign is beyond the scope of this paper. HOA typically correlates with black carbon, which is co-emitted by the same source; biomass burning correlates with the organic fragment at m/z 60 (org_{60}) which corresponds mainly to the ion $C_2H_4O_2^+$ and has been shown to be a good tracer for biomass burning (Alfarra et al., 2007; DeCarlo et al., 2008; Aiken et al., 2009). However, in marine environment, m/z 60 is usually dominated by $Na^{37}Cl$ (Ovadnevaite et al., 2012). To further evaluate the interpretation of primary sources within the selected solution, source-specific ratios can be calculated (e.g., HOA / CO, HOA/BC and HOA / NO_x) and compared with literature studies. However, in our work this approach could not be systematically applied due to the lack of external data. Bilinear regression (Allan et al., 2010) can be used to estimate these ratios also in the presence of multiple sources; however, this method is more applicable to a single data set rather than an overview of 25 data sets across Europe.

The secondary OA components are compared with the secondary inorganic species: the SV-OOA time series are expected to correlate with nitrate (NO_3) due to the higher volatility of this component and its partitioning behavior with temperature, while the LV-OOA time series are correlated with sulfate (SO_4) since it represents a less volatile fraction (Lanz et al., 2007). However, depending on the specific features of the SV-OOA and LV-OOA components, associated with their origin and processing in the atmosphere, their correlations with the secondary inorganic species might be not very high (Table S3). Finally, to further validate our source apportionment results, we investigated the diurnal pattern of the identified sources. In order to remove the effect of

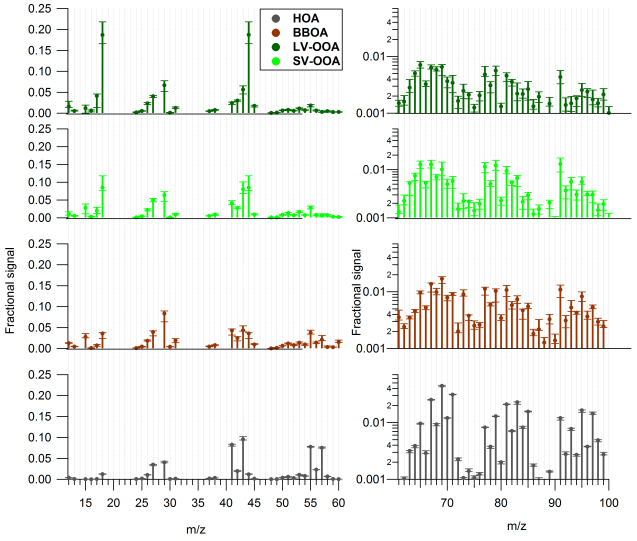

Figure 7. Mass spectral variability for the retrieved ME-2 OA sources. Median values are represented with circles and the 25th and 75th percentiles with error bars.

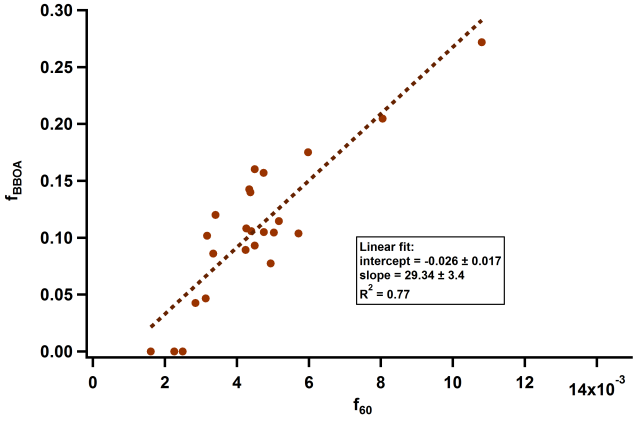

Figure 8. Average BBOA fractional contribution vs. average f_{60} for each site.

boundary layer height evolution, we recommend that users investigate the diurnal patterns of the relative source contributions relative source contribution diurnal pattern in addition to the absolute source contributions.

Figure 6 shows the diurnal patterns of HOA, BBOA, SV-OOA and LV-OOA. First, median diurnal patterns for each source referred to a specific site and campaign are evaluated; then mean values ($\pm$ standard deviation) for the three campaign periods are calculated and reported in Fig. 6. Two peaks corresponding to rush hour times are observed for the HOA daily pattern, while an increasing contribution in the evening hours is typical for BBOA emissions. A rather flat pattern is shown for LV-OOA, although an afternoon increase can be observed for the late spring 2008 campaigns similarly to the expected summertime behavior. Finally, an anti-correlated pattern with temperature is found for SV-OOA. Figure 6 does not report the diurnal pattern of the cooking source since it is identified only for the urban site of Barcelona. The reader should refer to Fig. 3 for the validation of the COA diurnal pattern which is characterized by two peaks corresponding to the meal hours.

4.3 POA and SOA mass spectral variability

Figure 7 shows the median mass spectra of HOA (n=25), BBOA ($n = 22$), SV-OOA ($n = 21$) and LV-OOA ($n = 25$) together with the 25th and 75th percentiles. The presented mass spectra (MS) can be considered as reference profiles for European sites in addition to the work presented by Ng et al. (2011a), where only for a reduced number of data sets it was possible to retrieve a good separation of primary sources (e.g., HOA and BBOA). The comparison between the Ng et al. (2011a) MS and our median profiles provides an R^2 equal to 0.99, 0.93, 0.86 and 0.95 for HOA, BBOA, SV-OOA and LV-OOA, respectively. However, as shown in Fig. 6, specific m/z express a stronger variability within a source profile compared to others, as later discussed later.

The hydrocarbon-like OA (HOA) profile is characterized by peaks corresponding to aliphatic hydrocarbons (including m/z 27, 41, 43, 55, 57, 69, 71, etc.) (Canagaratna et al., 2004). Since this mass spectrum is strongly constrained when running the ME-2 algorithm (a value=0.05), the site to site variability of the characteristic peaks is reduced, as shown by the percentiles in Fig. 7. However, we do not expect this source to significantly vary in terms of MS as demonstrated by the comparison of HOA mass spectra retrieved from ambient measurements (e.g., $R^2 = 0.99$ between the average HOA MS from Ng et al. (2011a) and the HOA MS retrieved in Paris (Crippa et al., 2013)) and laboratory experiments (Mohr et al., 2009).

On the contrary, as discussed previously (Grieshop et al., 2009; Heringa et al., 2011), the biomass burning mass spectrum is strongly affected by the type of wood, burning conditions, etc., and thus highly variable. For this reason the reference spectrum of BBOA is not constrained very strongly when running the ME-2 model, but we adopt an a value of 0.3 to account for this variability. The characteristic peaks of this source profile are m/z 29 (CHO^+), 60 ($C_2H_4O_2^+$), 73 ($C_3H_5O_2^+$) which are associated with fragmentation of anhydrosugars such as levoglucosan (Alfarra et al., 2007; Aiken et al., 2009). Major differences in the primary OA mass spectra are observed at m/z 29, 44 and higher masses (e.g., m/z 67, 69, 73, 77, 79, 81, 91).

For the secondary components the major variability is associated with the f_{44} to f_{43} ratio which provides information about the degree of oxygenation of the considered factor. The LV-OOA factor is characterized by an average f_{44} to f_{43} ratio equal to 3.3, corresponding to highly oxygenated compounds, while the SV-OOA has a lower ratio (on average equal to 1.1). The f_{44} vs. f_{43} information is also summarized

in Fig. S4, where the SV- and LV-OOA components retrieved for all our data sets are represented within the triangular space defined by Ng et al. (2010). The aging of secondary OA components can be studied considering the evolution in the f_{44} (corresponding to the CO_2^+ ion) vs. f_{43} (mostly corresponding to the $C_2H_3O^+$ ion) space.

The relative fractions of specific m/z are different between these two secondary components. A comparison of the median SV- and LV-OOA MS reveals that: m/z 91, 105, 107, 109, 115, 117, and 119 are much higher in the SV-OOA MS than in the LV-OOA, while m/z 45, 100, 101, 113 are higher in the LV-OOA MS than in the SV-OOA. This comparison is performed on the normalized spectra from m/z 45 up to 200. No specific tracers for the two components are retrieved in our study.

Using the equation introduced by Aiken et al. (2008) it is possible to estimate the degree of oxygenation of each source making use of the linear relation between the O : C ratio and the fraction of m/z44 of a specific factor. The resulting O : C ratio is 0.13 for HOA, 0.22 for BBOA, 0.41 for SV-OOA and 0.81 for LV-OOA, consistently with AMS high resolution analyses available in the literature (Jimenez et al., 2009; Ng et al., 2010; DeCarlo et al., 2010).

4.4 Assessment of the BBOA presence

Figure 8 reports the average fraction of BBOA to the total OA for each site as a function of the average f_{60} contribution. For only 3 locations it is not possible to identify a BBOA source, coherently with their corresponding f_{60} values below background level (which is expected to be around 0.3 %) (Cubison et al., 2011). A linear relation is found between f_{BBOA} and f_{60} (intercept = -0.026, slope=29.34), with an R^2 equal to 0.77, representing the possibility to estimate the amount of BBOA contributing to a site based on the f_{60} metric, even before performing a constrained/unconstrained positive matrix factorization run.

For a few sites with an f_{60} contribution close to the background level a small contribution of BBOA to total OA (4 %) is found, representing the uncertainty of our approach, but also to the f_{60} background level variability associated with different sites and to the deployment of different AMS. However, in this study the source apportionment including BBOA relies not only on f_{60}, but on all mass fragments.

Finally, high BBOA contributions are also observed during rather warm periods (e.g., during the spring 2008 campaign in Helsinki, San Pietro Capofiume, Cabauw) when the domestic heating is not expected. Probable but uncertain sources include open fires, agricultural waste disposal, forest and gardening waste burning which often show their maximum contributions during spring and autumn.

4.5 Sensitivity analysis of the *a* value approach

In order to further evaluate our source apportionment results, we perform a sensitivity analysis varying the a value for the HOA MS, to loosen the constraint for this source and subsequently provide a range of possible reasonable solutions. The HOA MS is initially constrained with an a value of 0.05 because we do not expect it to vary a lot from site to site, as previously discussed. However, releasing the constraint associated with the a value, it is still possible to separate the traffic source for all the sites. Several a value runs are performed increasing its value until the HOA source is not meaningful anymore, based on the features of the HOA MS (e.g., a too high contribution of m/z 44 represented a mixture of HOA with BBOA or secondary oxygenated sources), the variation in the HOA diurnal pattern and, when available, the correlation with external data. For most of the sites an upper range of the a value is found to be 0.2, in accordance with Canonaco et al. (2013) who identified an upper limit of 0.15 for the HOA MS at the urban background site in Zurich for a longer time period.

Table 3 summarizes our sensitivity analysis results, reporting for each site the relative contribution of the retrieved OA sources within the a value range of 0.05–0.2 for the HOA MS. The HOA relative contribution does not vary significantly (only by a few percent) within the considered a value range and is sometimes associated with the reapportionment of the other sources (e.g., the contribution of the SV-OOA factor varied accordingly).

Concerning BBOA, an a value of 0.3 is found to give reasonable freedom to the BBOA MS in the ME-2 model, while it is not possible to define a consistent a value upper limit for all the sites. In fact it is difficult to define a criterion to determine when the BBOA factor fails when increasing the a value, due to the variable features of the BBOA MS and the lack of stronger metrics in this study. In our study we present a sensitivity test for BBOA varying the a value in the range 0.2–0.4 and we report the relative contribution of OA sources to total organic as a function of the a value extremes of the investigated range (refer to Table 4). However, if a priori knowledge about wood burning conditions is available for a site, we suggest to constrain the BBOA MS deriving from the same kind of burning conditions, instead of using an average BBOA MS.

Finally, we recognize that the selection of the reference mass spectra to be constrained when running the ME-2 approach is critical and it might affect the source apportionment output. Therefore, in Sect. 6 of the Supplementary Material, the effect of the choice of specific mass spectrum as reference when running ME-2 on the source apportionment output is investigated. However, a future study using more suited data sets with more external constraints on the validity of the retrieved sources will be performed to fully address this important task.

Table 3. Sensitivity analysis for the HOA factor (*a* value range=0-0.2, *a* value for BBOA=0.3 if constrained). The relative contribution of OA sources to the total OA is reported varying the HOA *a* value.

site	HOA	BBOA	SV-OOA	LV-OOA	COA	MSA
BCN	0.24–0.25	0.09–0.07	0.13–0.10	0.37–0.34	0.17–0.24	–
CBW	0.14–0.16	0.10–0.10	0.23–0.22	0.38–0.38	–	–
	0.17–0.21	0.09–0.11	0.31–0.34	0.43–0.34	–	–
FKL	0.04–0.05	–	0.23–0.28	0.68–0.64	–	0.05–0.03
HEL	0.16–0.16	0.15–0.15	0.31–0.18	0.38–0.51	–	–
SMR	0.06–0.07	0.04–0.05	0.37–0.34	0.53–0.54	–	–
	0.03–0.04	0.05–0.05	0.29–0.31	0.63–0.60	–	–
JFJ	0.07–0.07	0.11–0.12	–	0.82–0.81	–	–
KPO	0.11–0.17	0.13–0.10	0.35–0.34	0.41–0.39	–	–
MH	0.11–0.14	0.16–0.13	0.25–0.30	0.41–0.36	–	0.07–0.07
	0.11–0.15	0.30–0.27	–	0.57–0.55	–	0.02–0.02
MPZ	0.07–0.06	–	0.37–0.34	0.56–0.60	–	–
	0.08–0.08	0.14–0.15	0.34–0.31	0.44–0.46	–	–
	0.10–0.10	0.17–0.10	0.30–0.28	0.43–0.52	–	–
MSY	0.13–0.09	0.10–0.10	–	0.77–0.81	–	–
PAY	0.05–0.07	0.11–0.11	0.29–0.29	0.54–0.53	–	–
	0.07–0.08	0.10–0.10	0.26–0.22	0.57–0.60	–	–
PUI	0.21–0.27	–	–	0.79–0.73	–	–
PDD	0.01–0.02	0.09–0.08	0.20–0.20	0.70–0.70	–	–
	0.05–0.05	0.17–0.17	0.37–0.37	0.41–0.41	–	–
SPC	0.09–0.12	0.16–0.18	0.26–0.24	0.49–0.46	–	–
VAV	0.20–0.22	0.13–0.13	–	0.67–0.65	–	–
	0.10–0.13	0.15–0.16	0.26–0.20	0.49–0.51	–	–
CHL	0.16–0.18	0.16–0.15	0.22–0.21	0.46–0.46	–	–
HAR	0.09–0.15	0.11–0.08	0.31–0.30	0.49–0.47	–	–

Table 4. Sensitivity analysis for the BBOA factor (*a* value range=0.2-0.4, *a* value for HOA=0.05). The relative contribution of OA sources to the total OA is reported varying the BBOA *a* value. In the table, the first number refers to the solution obtained with an *a* value of 0.2 and the second one to with *a* value of 0.4.

site	HOA	BBOA	SV-OOA	LV-OOA	COA	MSA
BCN	0.25–0.25	0.07–0.08	0.12–0.11	0.39–0.41	0.16–0.15	–
CBW	0.09–0.07	0.08–0.10	0.17–0.19	0.66–0.65	–	–
	0.20–0.19	0.10–0.10	0.33–0.34	0.36–0.36	–	–
SMR	0.06–0.06	0.04–0.05	0.55–0.50	0.36–0.38	–	–
	0.03–0.03	0.04–0.05	0.39–0.26	0.54–0.66	–	–
JFJ	0.08–0.07	0.10–0.12	–	0.82–0.81	–	–
KPO	0.12–0.11	0.10–0.14	0.33–0.35	0.45–0.39	–	–
MH	0.11–0.11	0.14–0.15	0.24–0.15	0.44–0.52	–	0.07–0.07
	0.13–0.13	0.27–0.32	–	0.59–0.54	–	0.01–0.02
MSY	0.12–0.12	0.09–0.13	–	0.78–0.75	–	–
PAY	0.06–0.05	0.10–0.10	0.27–0.35	0.58–0.49	–	–
	0.08–0.08	0.10–0.09	0.26–0.20	0.57–0.63	–	–
PDD	0.01–0.01	0.08–0.09	0.45–0.466	0.45–0.44	–	–
	0.05–0.05	0.15–0.18	0.36–0.37	0.44–0.40	–	–
SPC	0.11–0.09	0.15–0.20	0.28–0.21	0.46–0.50	–	–
VAV	0.20–0.21	0.15–0.13	–	0.65–0.67	–	–
	0.12–0.11	0.14–0.18	0.20–0.22	0.54–0.50	–	–
HAR	0.07–0.09	0.12–0.10	0.44–0.45	0.36–0.37	–	–

5 Conclusions

We developed a new standardized approach for source apportionment analysis applicable for aerosol mass spectrometer measurements. Our source apportionment procedure was tested and systematically applied to 25 organic aerosol data sets, demonstrating the possibility to separate the main primary and secondary organic aerosol components also for rural sites. This represents a significant advancement compared to previous literature studies which showed limitations of the unconstrained positive matrix factorization when applied on rural/background site data sets. Our source apportionment strategy is significantly improved through the use of the multilinear engine (Paatero, 1999) and the SoFi toolkit developed by Canonaco et al. (2013). Future applications of our strategy are associated not only with the unit mass resolution aerosol mass spectrometer, but also the high resolution instruments and the aerosol chemical speciation monitor. In the next few years the latter will provide a network of long-term online data about the aerosol chemical composition, often measured at non-urban locations. The investigation of OA sources will require guidelines to overcome instrument-and data-related limitations. This paper provides these guidelines with a structured methodology for a consistent interpretation of OA source apportionment work.

Moreover, with our study we are able to describe organic aerosol sources all over Europe, thus improving the actual knowledge on the OA source distribution and representing an important step in the definition of mitigation strategies at the regional scale.

On average primary sources contribute less than 30 % to the total OA mass concentration, while the predominant fraction of OA is associated with secondary formation (mainly SV-OOA and LV-OOA). The traffic contribution is season independent and represents 11 ± 6 % of total OA all over Europe. Biomass burning represents 12 ± 5 % of the total OA mass and might be associated with domestic heating during wintertime and to open fires, agricultural waste disposal, waste burning etc., during the other seasons. Cooking is indeed a relevant source mainly for urban locations (15 %). The control of primary organic aerosol emissions should be performed together with the reduction of the sources of secondary OA (SV- and LV-OOA) in Europe as the latter make the dominant OA fraction, although this task is quite challenging. Finally, coupling European wide measurements and source apportionment results with regional and global models will improve their prediction of POA and SOA components.

The Supplement related to this article is available online at doi:10.5194/acp-14-6159-2014-supplement.

Acknowledgements. This work was funded through the European EUCAARI IP, other collaborating initiatives and through national funding through individual members states to the CLRTAP (Convention on Long-range Transboundary Air Pollution) as a contribution to the EMEP monitoring program. The CEH (Centre for Ecology & Hydrology) and UK contribution, including much of the synthesizing analysis, was funded by the UK Department for Environment, Food and Rural Affairs (Defra). Measurements were further funded by the following national sources: the Spanish Ministry of Science and Innovation, the Swiss Federal Office for Environment, Helsinki Energy, the Ministry of Transport and Communications Finland, the Academy of Finland Center of Excellence Program (project no. 1118615), the German Umweltbundesamt (contracts 351 01 031 & 038), the Swedish Research Council and Swedish Environmental Protection Agency, as well as the Nordic Council of Ministers. Several groups were supported by the EU ACCENT NoE and several sites by the EUSAAR (European Supersites for Atmospheric Aerosol Research) Infrastructure Network. The Chilbolton data set was supported by the UK Natural Environment Research Council (NERC) through the Aerosol Interactions in Mixed Phase Clouds project [Grant ref: NE/E01125X/1], part of the APPRAISE directed program.

The K-Puszta measurements were supported by the access to infrastructures fund of the EU FP6 ACCENT network of excellence. DAD and JLJ acknowledge support from NSF AGS-1243354, NOAA NA13OAR4310063 and DOE (BER/ASR) DE-SC0006035 and DE-SC0011105.

Edited by: A. Nenes

References

Aas, W., Tsyro, S., Bieber, E., Bergström, R., Ceburnis, D., Ellermann, T., Fagerli, H., Frölich, M., Gehrig, R., Makkonen, U., Nemitz, E., Otjes, R., Perez, N., Perrino, C., Prévôt, A. S. H., Putaud, J.-P., Simpson, D., Spindler, G., Vana, M., and Yttri, K. E.: Lessons learnt from the first EMEP intensive measurement periods, Atmos. Chem. Phys., 12, 8073–8094, doi:10.5194/acp-12-8073-2012, 2012.

Aiken, A. C., Decarlo, P. F., Kroll, J. H., Worsnop, D. R., Huffman, J. A., Docherty, K. S., Ulbrich, I. M., Mohr, C., Kimmel, J. R., Sueper, D., Sun, Y., Zhang, Q., Trimborn, A., Northway, M., Ziemann, P. J., Canagaratna, M. R., Onasch, T. B., Alfarra, M. R., Prevot, A. S. H., Dommen, J., Duplissy, J., Metzger, A., Baltensperger, U., and Jimenez, J. L.: O/C and OM/OC ratios of primary, secondary, and ambient organic aerosols with high-resolution time-of-flight aerosol mass spectrometry, Environ. Sci. Technol., 42, 4478–4485, 2008.

Aiken, A. C., Salcedo, D., Cubison, M. J., Huffman, J. A., DeCarlo, P. F., Ulbrich, I. M., Docherty, K. S., Sueper, D., Kimmel, J. R., Worsnop, D. R., Trimborn, A., Northway, M., Stone, E. A., Schauer, J. J., Volkamer, R. M., Fortner, E., de Foy, B., Wang, J., Laskin, A., Shutthanandan, V., Zheng, J., Zhang, R., Gaffney, J., Marley, N. A., Paredes-Miranda, G., Arnott, W. P., Molina, L. T., Sosa, G., and Jimenez, J. L.: Mexico City aerosol analysis during MILAGRO using high resolution aerosol mass spectrometry at the urban supersite (T0) - Part 1: Fine particle composition and organic source apportionment, Atmos. Chem. and Phys., 9, 6633–6653, doi:10.5194/acp-9-6633-2009, 2009.

Alfarra, M. R., Prevot, A. S. H., Szidat, S., Sandradewi, J., Weimer, S., Lanz, V. A., Schreiber, D., Mohr, M., and Baltensperger, U.: Identification of the mass spectral signature of organic aerosols from wood burning emissions, Environ. Sci. Technol., 41, 5770–5777, 2007.

Allan, J. D., Delia, A. E., Coe, H., Bower, K. N., Alfarra, M. R., Jimenez, J. L., Middlebrook, A. M., Drewnick, F., Onasch, T. B., Canagaratna, M. R., Jayne, J. T., and Worsnop, D. R.: A generalised method for the extraction of chemically resolved mass spectra from Aerodyne aerosol mass spectrometer data, J. Aerosol Sci., 35, 909–922, 2004.

Allan, J. D., Williams, P. I., Morgan, W. T., Martin, C. L., Flynn, M. J., Lee, J., Nemitz, E., Phillips, G. J., Gallagher, M. W., and Coe, H.: Contributions from transport, solid fuel burning and cooking to primary organic aerosols in two UK cities, Atmos. Chem. Phys., 10, 647–668, doi:10.5194/acp-10-647-2010, 2010.

Brown, S. G., Lee, T., Norris, G. A., Roberts, P. T., Collett, J. L., Paatero, P., and Worsnop, D. R.: Receptor modeling of near-roadway aerosol mass spectrometer data in Las Vegas, Nevada, with EPA PMF, Atmos. Chem. Phys., 12, 309–325, doi:10.5194/acp-12-309-2012, 2012.

Canagaratna, M. R., Jayne, J. T., Ghertner, D. A., Herndon, S., Shi, Q., Jimenez, J. L., Silva, P. J., Williams, P., Lanni, T., Drewnick, F., Demerjian, K. L., Kolb, C. E., and Worsnop, D. R.: Chase studies of particulate emissions from in-use New York City vehicles, Aerosol Sci. Technol., 38, 555–573, 2004.

Canonaco, F., Crippa, M., Slowik, J. G., Baltensperger, U., and Prévôt, A. S. H.: SoFi, an Igor based interface for the efficient use of the generalized multilinear engine (ME-2) for source apportionment: application to aerosol mass spectrometer data, Atmos. Meas. Tech., 6 3649–3661, doi:10.5194/amt-6-3649-2013, 2013.

Canonaco, F., Baltensperger, U., and Prévôt, A. S. H.: Sensitivity analysis in ME-2 with the toolkit SoFi: Testing various primary and secondary AMS literature profiles, in preparation, 2014a.

Canonaco, F., Crippa, M., Baltensperger, U., and Prévôt, A. S. H.: Development of the pulling technique within the ME-2 solver using SoFi, in preparation, 2014b.

Carbone, S., Aurela, M., Saarnio, K., Saarikoski, S., Frey, A., Sueper, D., Ulbrich, I. M., Jimenez, J. L., Kulmala, M., Worsnop, D. R., and Hillamo, R.: Wintertime aerosol chemistry in sub-Arctic urban air, Aerosol Sci. Technol., 48, 313–323, 2014.

Crippa, M., DeCarlo, P. F., Slowik, J. G., Mohr, C., Heringa, M. F., Chirico, R., Poulain, L., Freutel, F., Sciare, J., Cozic, J., Di Marco, C. F., Elsasser, M., José, N., Marchand, N., Abidi, E., Wiedensohler, A., Drewnick, F., Schneider, J., Borrmann, S., Nemitz, E., Zimmermann, R., Jaffrezo, J.-L., Prévôt, A. S. H., and Baltensperger, U.: Wintertime aerosol chemical composition and source apportionment of the organic fraction in the metropolitan area of Paris, Atmos. Chem. Phys., 13, 961–981, doi:10.5194/acp-13-961-2013, 2013.

Cubison, M. J., Ortega, A. M., Hayes, P. L., Farmer, D. K., Day, D., Lechner, M. J., Brune, W. H., Apel, E., Diskin, G. S., Fisher, J. A., Fuelberg, H. E., Hecobian, A., Knapp, D. J., Mikoviny, T., Riemer, D., Sachse, G. W., Sessions, W., Weber, R. J., Weinheimer, A. J., Wisthaler, A., and Jimenez, J. L.: Effects of aging on organic aerosol from open biomass burning smoke in aircraft and laboratory studies, Atmos. Chem. Phys., 11, 12049–12064, doi:10.5194/acp-11-12049-2011, 2011.

Dall'Osto, M., Ceburnis, D., Martucci, G., Bialek, J., Dupuy, R., Jennings, S. G., Berresheim, H., Wenger, J., Healy, R., Facchini, M. C., Rinaldi, M., Giulianelli, L., Finessi, E., Worsnop, D., Ehn, M., Mikkila, J., Kulmala, M., and O'Dowd, C. D.: Aerosol properties associated with air masses arriving into the North East Atlantic during the 2008 Mace Head EUCAARI intensive observing period: an overview, Atmos. Chem. Phys., 10, 8413–8435, doi:10.5194/acp-10-8413-2010, 2010.

De Gouw, J. and Jimenez, J. L.: Organic aerosols in the Earth's atmosphere, Environ. Sci. Technol., 43, 7614–7618, 2009.

DeCarlo, P. F., Kimmel, J. R., Trimborn, A., Northway, M. J., Jayne, J. T., Aiken, A. C., Gonin, M., Fuhrer, K., Horvath, T., Docherty, K. S., Worsnop, D. R., and Jimenez, J. L.: Field-deployable, high-resolution, time-of-flight aerosol mass spectrometer, Anal. Chem., 78, 8281–8289, 2006.

DeCarlo, P. F., Dunlea, E. J., Kimmel, J. R., Aiken, A. C., Sueper, D., Crounse, J., Wennberg, P. O., Emmons, L., Shinozuka, Y., Clarke, A., Zhou, J., Tomlinson, J., Collins, D. R., Knapp, D., Weinheimer, A. J., Montzka, D. D., Campos, T., and Jimenez, J. L.: Fast airborne aerosol size and chemistry measurements above Mexico City and Central Mexico during the MILAGRO campaign, Atmos. Chem. Phys., 8, 4027–4048, doi:10.5194/acp-8-4027-2008, 2008.

DeCarlo, P. F., Ulbrich, I. M., Crounse, J., de Foy, B., Dunlea, E. J., Aiken, A. C., Knapp, D., Weinheimer, A. J., Campos, T., Wennberg, P. O., and Jimenez, J. L.: Investigation of the sources and processing of organic aerosol over the Central Mexican Plateau from aircraft measurements during MILAGRO, Atmos. Chem. Phys., 10, 5257–5280, doi:10.5194/acp-10-5257-2010, 2010.

Drewnick, F., Hings, S. S., DeCarlo, P., Jayne, J. T., Gonin, M., Fuhrer, K., Weimer, S., Jimenez, J. L., Demerjian, K. L., Borrmann, S., and Worsnop, D. R.: A new time-of-flight aerosol mass spectrometer (TOF-AMS) – Instrument description and first field deployment, Aerosol Sci. Technol., 39, 637–658, 2005.

Fountoukis, C., Racherla, P. N., van der Gon, H. A. C. D., Polymeneas, P., Charalampidis, P. E., Pilinis, C., Wiedensohler, A., Dall'Osto, M., O'Dowd, C., and Pandis, S. N.: Evaluation of a three-dimensional chemical transport model (PMCAMx) in the European domain during the EUCAARI May 2008 campaign, Atmos. Chem. Phys., 11, 10331–10347, doi:10.5194/acp-11-10331-2011, 2011.

Freney, E. J., Sellegri, K., Canonaco, F., Boulon, J., Hervo, M., Weigel, R., Pichon, J. M., Colomb, A., Prevot, A. S. H., and Laj, P.: Seasonal variations in aerosol particle composition at the puy-de-Dome research station in France, Atmos. Chem. Phys., 11, 13047–13059, doi:10.5194/acp-11-13047-2011, 2011.

Fröhlich, R., Cubison, M. J., Slowik, J. G., Bukowiecki, N., Prévôt, A. S. H., Baltensperger, U., Schneider, J., Kimmel, J. R., Gonin, M., Rohner, U., Worsnop, D. R., and and Jayne, J. T.: The ToF-ACSM: a portable aerosol chemical speciation monitor with TOFMS detection, Atmos. Meas. Tech., 6, 3225–3241, doi:10.5194/amt-6-3225-2013, 2013.

Grieshop, A. P., Donahue, N. M., and Robinson, A. L.: Laboratory investigation of photochemical oxidation of organic aerosol from wood fires 2: analysis of aerosol mass spectrometer data, Atmos. Chem. Phys., 9, 2227–2240, doi:10.5194/acp-9-2227-2009, 2009.

Hallquist, M., Wenger, J. C., Baltensperger, U., Rudich, Y., Simpson, D., Claeys, M., Dommen, J., Donahue, N. M., George, C., Goldstein, A. H., Hamilton, J. F., Herrmann, H., Hoffmann, T., Iinuma, Y., Jang, M., Jenkin, M. E., Jimenez, J. L., Kiendler-Scharr, A., Maenhaut, W., McFiggans, G., Mentel, T. F., Monod, A., Prevot, A. S. H., Seinfeld, J. H., Surratt, J. D., Szmigielski, R., and Wildt, J.: The formation, properties and impact of secondary organic aerosol: current and emerging issues, Atmos. Chem. Phys., 9, 5155–5236, doi:10.5194/acp-9-5155-2009, 2009.

Hao, L., Romakkaniemi, S., Kortelainen, A., Jaatinen, A., Portin, H., Miettinen, P., Komppula, M., Leskinen, A., Virtanen, A., Smith, J. N., Sueper, D., Worsnop, D. R., Lehtinen, K. E. J., and Laaksonen, A.: Aerosol chemical composition in cloud events by high resolution time-of-flight aerosol mass spectrometry, Environ. Sci. Technol., 47, 2645–2653, doi:10.1021/es302889w, 2013.

Heringa, M. F., DeCarlo, P. F., Chirico, R., Tritscher, T., Dommen, J., Weingartner, E., Richter, R., Wehrle, G., Prévôt, A. S. H., and Baltensperger, U.: Investigations of primary and secondary particulate matter of different wood combustion appliances with a high-resolution time-of-flight aerosol mass spectrometer, Atmos. Chem. Phys., 11, 5945–5957, doi:10.5194/acp-11-5945-2011, 2011.

Hildebrandt, L., Engelhart, G. J., Mohr, C., Kostenidou, E., Lanz, V. A., Bougiatioti, A., DeCarlo, P. F., Prevot, A. S. H., Baltensperger, U., Mihalopoulos, N., Donahue, N. M., and Pandis, S. N.: Aged organic aerosol in the Eastern Mediterranean: the Finokalia Aerosol Measurement Experiment-2008, Atmos. Chem. Phys., 10, 4167–4186, doi:10.5194/acp-10-4167-2010, 2010a.

Hildebrandt, L., Kostenidou, E., Mihalopoulos, N., Worsnop, D. R., Donahue, N. M., and Pandis, S. N.: Formation of highly oxygenated organic aerosol in the atmosphere: Insights from the Finokalia Aerosol Measurement Experiments, Geophys. Res. Lett., 37, L23801, doi:10.1029/2010GL045193, 2010b.

Hildebrandt, L., Kostenidou, E., Lanz, V. A., Prevot, A. S. H., Baltensperger, U., Mihalopoulos, N., Laaksonen, A., Donahue, N. M., and Pandis, S. N.: Sources and atmospheric processing of organic aerosol in the Mediterranean: insights from aerosol mass spectrometer factor analysis, Atmos. Chem. Phys., 11, 12499–12515, doi:10.5194/acp-11-12499-2011, 2011.

IPCC: Fourth assessment report: The physical science basis, working group I, Final report, Geneva, Switzerland, available at: http://www.ipcc.ch/ipccreports/ar4-wg1.htm, 2007., 2007.

Jayne, J. T., Leard, D. C., Zhang, X. F., Davidovits, P., Smith, K. A., Kolb, C. E., and Worsnop, D. R.: Development of an aerosol mass spectrometer for size and composition analysis of submicron particles, Aerosol Sci. Technol., 33, 49–70, 2000.

Jimenez, J. L., Canagaratna, M. R., Donahue, N. M., Prevot, A. S. H., Zhang, Q., Kroll, J. H., DeCarlo, P. F., Allan, J. D., Coe, H., Ng, N. L., Aiken, A. C., Docherty, K. S., Ulbrich, I. M., Grieshop, A. P., Robinson, A. L., Duplissy, J., Smith, J. D., Wilson, K. R., Lanz, V. A., Hueglin, C., Sun, Y. L., Tian, J., Laaksonen, A., Raatikainen, T., Rautiainen, J., Vaattovaara, P., Ehn, M., Kulmala, M., Tomlinson, J. M., Collins, D. R., Cubison, M. J., Dunlea, E. J., Huffman, J. A., Onasch, T. B., Alfarra, M. R., Williams, P. I., Bower, K., Kondo, Y., Schneider, J., Drewnick, F., Borrmann, S., Weimer, S., Demerjian, K., Salcedo, D., Cottrell, L., Griffin, R., Takami, A., Miyoshi, T., Hatakeyama, S., Shimono, A., Sun, J. Y., Zhang, Y. M., Dzepina, K., Kimmel, J. R., Sueper, D., Jayne, J. T., Herndon, S. C., Trimborn, A. M., Williams, L. R., Wood, E. C., Middlebrook, A. M., Kolb, C. E., Baltensperger, U., and Worsnop, D. R.: Evolution of organic aerosols in the atmosphere, Science, 326, 1525–1529, 2009.

Kanakidou, M., Seinfeld, J. H., Pandis, S. N., Barnes, I., Dentener, F. J., Facchini, M. C., Van Dingenen, R., Ervens, B., Nenes, A., Nielsen, C. J., Swietlicki, E., Putaud, J. P., Balkanski, Y., Fuzzi, S., Horth, J., Moortgat, G. K., Winterhalter, R., Myhre, C. E. L., Tsigaridis, K., Vignati, E., Stephanou, E. G., and Wilson, J.: Organic aerosol and global climate modelling: a review, Atmos. Chem. Phys., 5, 1053–1123, doi:10.5194/acp-5-1053-2005, 2005.

Knote, C., Brunner, D., Vogel, H., Allan, J., Asmi, A., Aijala, M., Carbone, S., van der Gon, H. D., Jimenez, J. L., Kiendler-Scharr, A., Mohr, C., Poulain, L., Prevot, A. S. H., Swietlicki, E., and Vogel, B.: Towards an online-coupled chemistry-climate model: evaluation of trace gases and aerosols in COSMO-ART, Geosci. Model Dev., 4, 1077–1102, doi:10.5194/gmd-4-1077-2011, 2011.

Kulmala, M., Asmi, A., Lappalainen, H. K., Carslaw, K. S., Poschl, U., Baltensperger, U., Hov, O., Brenquier, J. L., Pandis, S. N., Facchini, M. C., Hansson, H. C., Wiedensohler, A., and O'Dowd, C. D.: Introduction: European Integrated Project on Aerosol Cloud Climate and Air Quality interactions (EUCAARI) – integrating aerosol research from nano to global scales, Atmos. Chem. Phys., 9, 2825–2841, doi:10.5194/acp-5-1053-2005, 2009.

Kulmala, M., Asmi, A., Lappalainen, H. K., Baltensperger, U., Brenguier, J. L., Facchini, M. C., Hansson, H. C., Hov, O., O'Dowd, C. D., Poschl, U., Wiedensohler, A., Boers, R., Boucher, O., de Leeuw, G., van der Gon, H. A. C. D., Feichter, J., Krejci, R., Laj, P., Lihavainen, H., Lohmann, U., McFiggans, G., Mentel, T., Pilinis, C., Riipinen, I., Schulz, M., Stohl, A., Swietlicki, E., Vignati, E., Alves, C., Amann, M., Ammann, M., Arabas, S., Artaxo, P., Baars, H., Beddows, D. C. S., Bergstrom, R., Beukes, J. P., Bilde, M., Burkhart, J. F., Canonaco, F., Clegg, S. L., Coe, H., Crumeyrolle, S., D'Anna, B., Decesari, S., Gilardoni, S., Fischer, M., Fjaeraa, A. M., Fountoukis, C., George, C., Gomes, L., Halloran, P., Hamburger, T., Harrison, R. M., Herrmann, H., Hoffmann, T., Hoose, C., Hu, M., Hyvarinen, A., Horrak, U., Iinuma, Y., Iversen, T., Josipovic, M., Kanakidou, M., Kiendler-Scharr, A., Kirkevåg, A., Kiss, G., Klimont, Z., Kolmonen, P., Komppula, M., Kristjansson, J. E., Laakso, L., Laaksonen, A., Labonnote, L., Lanz, V. A., Lehtinen, K. E. J., Rizzo, L. V., Makkonen, R., Manninen, H. E., McMeeking, G., Merikanto, J., Minikin, A., Mirme, S., Morgan, W. T., Nemitz, E., O'Donnell, D., Panwar, T. S., Pawlowska, H., Petzold, A., Pienaar, J. J., Pio, C., Plass-Duelmer, C., Prévôt, A. S. H., Pryor, S., Reddington, C. L., Roberts, G., Rosenfeld, D., Schwarz, J., Seland, O., Sellegri, K., Shen, X. J., Shiraiwa, M., Siebert, H., Sierau, B., Simpson, D., Sun, J. Y., Topping, D., Tunved, P., Vaattovaara, P., Vakkari, V., Veefkind, J. P., Visschedijk, A., Vuollekoski, H., Vuolo, R., Wehner, B., Wildt, J., Woodward, S., Worsnop, D. R., van Zadelhoff, G. J., Zardini, A. A., Zhang, K., van Zyl, P. G., Kerminen, V. M., Carslaw, K. S., and Pandis, S. N.: General overview: European Integrated project on Aerosol Cloud Climate and Air Quality interactions (EUCAARI) – integrating aerosol research from nano to global

scales, Atmos. Chem. Phys., 11, 13061–13143, doi:10.5194/acp-11-13061-2011, 2011.

Lanz, V. A., Alfarra, M. R., Baltensperger, U., Buchmann, B., Hueglin, C., and Prevot, A. S. H.: Source apportionment of submicron organic aerosols at an urban site by factor analytical modelling of aerosol mass spectra, Atmos. Chem. Phys., 7, 1503–1522, doi:10.5194/acp-7-1503-2007, 2007.

Lanz, V. A., Alfarra, M. R., Baltensperger, U., Buchmann, B., Hueglin, C., Szidat, S., Wehrli, M. N., Wacker, L., Weimer, S., Caseiro, A., Puxbaum, H., and Prevot, A. S. H.: Source attribution of submicron organic aerosols during wintertime inversions by advanced factor analysis of aerosol mass spectra, Environ. Sci. Technol., 42, 214–220, 2008.

Lanz, V. A., Prevot, A. S. H., Alfarra, M. R., Weimer, S., Mohr, C., DeCarlo, P. F., Gianini, M. F. D., Hueglin, C., Schneider, J., Favez, O., D'Anna, B., George, C., and Baltensperger, U.: Characterization of aerosol chemical composition with aerosol mass spectrometry in Central Europe: an overview, Atmos. Chem. Phys., 10, 10453–10471, doi:10.5194/acp-10-10453-2010, 2010.

Leskinen, A., Arola, A., Komppula, M., Portin, H., Tiitta, P., Miettinen, P., Romakkaniemi, S., Laaksonen, A., and Lehtinen, K. E. J.: Seasonal cycle and source analyses of aerosol optical properties in a semi-urban environment at Puijo station in Eastern Finland, Atmos. Chem. Phys., 12, 5647–5659, doi:10.5194/acp-12-5647-2012, 2012.

Li, Y. P., Elbern, H., Lu, K. D., Friese, E., Kiendler-Scharr, A., Mentel, T. F., Wang, X. S., Wahner, A., and and Zhang, Y. H.: Updated aerosol module and its application to simulate secondary organic aerosols during IMPACT campaign May 2008, Atmos. Chem. Phys., 13, 6289–6304, doi:10.5194/acp-5-6289-2013, 2013.

Mensah, A. A., Holzinger, R., Otjes, R., Trimborn, A., Mentel, T. F., ten Brink, H., Henzing, B., and Kiendler-Scharr, A.: Aerosol chemical composition at Cabauw, The Netherlands as observed in two intensive periods in May 2008 and March 2009, Atmos. Chem. Phys., 12, 4723–4742, doi:10.5194/acp-12-4723-2012, 2012.

Mohr, C., Huffman, J. A., Cubison, M. J., Aiken, A. C., Docherty, K. S., Kimmel, J. R., Ulbrich, I. M., Hannigan, M., and Jimenez, J. L.: Characterization of primary organic aerosol emissions from meat cooking, trash burning, and motor vehicles with high-resolution aerosol mass spectrometry and comparison with ambient and chamber observations, Environ. Sci. Technol., 43, 2443–2449, 2009.

Mohr, C., DeCarlo, P. F., Heringa, M. F., Chirico, R., Slowik, J. G., Richter, R., Reche, C., Alastuey, A., Querol, X., Seco, R., Peñuelas, J., Jiménez, J. L., Crippa, M., Zimmermann, R., Baltensperger, U., and Prévôt, A. S. H.: Identification and quantification of organic aerosol from cooking and other sources in Barcelona using aerosol mass spectrometer data, Atmos. Chem. Phys., 12, 1649–1665, doi:10.5194/acp-12-1649-2012, 2012.

Murphy, B. N., Donahue, N. M., Fountoukis, C., Dall'Osto, M., O'Dowd, C., Kiendler-Scharr, A., and Pandis, S. N.: Functionalization and fragmentation during ambient organic aerosol aging: application of the 2-D volatility basis set to field studies, Atmos. Chem. Phys., 12, 10797-10816, 2012, http://www.atmos-chem-phys.net/12/10797/2012/.

Nemitz, E.: A snapshot European climatology of submicron aerosol chemical composition derived from an aerosol mass spectrometer network, in preparation, 2014.

Ng, N. L., Canagaratna, M. R., Zhang, Q., Jimenez, J. L., Tian, J., Ulbrich, I. M., Kroll, J. H., Docherty, K. S., Chhabra, P. S., Bahreini, R., Murphy, S. M., Seinfeld, J. H., Hildebrandt, L., Donahue, N. M., DeCarlo, P. F., Lanz, V. A., Prevot, A. S. H., Dinar, E., Rudich, Y., and Worsnop, D. R.: Organic aerosol components observed in Northern Hemispheric datasets from aerosol mass spectrometry, Atmos. Chem. Phys., 10, 4625–4641, doi:10.5194/acp-5-4625-2010, 2010.

Ng, N. L., Canagaratna, M. R., Jimenez, J. L., Zhang, Q., Ulbrich, I. M., and Worsnop, D. R.: Real-time methods for estimating organic component mass concentrations from aerosol mass spectrometer data, Environ. Sci. Technol., 45, 910–916, 2011a.

Ng, N. L., Herndon, S. C., Trimborn, A., Canagaratna, M. R., Croteau, P. L., Onasch, T. B., Sueper, D., Worsnop, D. R., Zhang, Q., Sun, Y. L., and Jayne, J. T.: An aerosol chemical speciation monitor (ACSM) for routine monitoring of the composition and mass concentrations of ambient aerosol, Aerosol Sci. Technol., 45, 780–794, 2011b.

Ovadnevaite, J., Ceburnis, D., Canagaratna, M., Berresheim, H., Bialek, J., Martucci, G., Worsnop, D. R., and O'Dowd, C.: On the effect of wind speed on submicron sea salt mass concentrations and source fluxes, J. Geophys. Res., Atmos., 117, D16201, doi:10.1029/2011JD017379, 2012.

Paatero, P., and Tapper, U.: Positive matrix factorization – a non-negative factor model with optimal utilization of error-estimates of data values, Environmetrics, 5, 111–126, 1994.

Paatero, P.: The multilinear engine – A table-driven, least squares program for solving multilinear problems, including the n-way parallel factor analysis model, J. Comp. Graph. Stat., 8, 854–888, 1999.

Paatero, P., Hopke, P. K., Song, X. H., and Ramadan, Z.: Understanding and controlling rotations in factor analytic models, Chemom. Intell. Lab. Syst., 60, 253–264, 2002.

Paatero, P. and Hopke, P. K.: Discarding or downweighting high-noise variables in factor analytic models, Anal. Chim. Acta, 490, 277–289, 2003.

Paatero, P., and Hopke, P. K.: Rotational tools for factor analytic models, J. Chemom., 23, 91-100, 2009.

Paglione, M., Kiendler-Scharr, A., Mensah, A. A., Finessi, E., Giulianelli, L., Sandrini, S., Facchini, M. C., Fuzzi, S., Schlag, P., Piazzalunga, A., Tagliavini, E., Henzing, J. S., and Decesari, S.: Identification of humic-like substances (HULIS) in oxygenated organic aerosols using NMR and AMS factor analyses and liquid chromatographic techniques, Atmos. Chem. Phys., 14, 25–45, doi:10.5194/acp-14-25-2014, 2014.

Pope, C. A. and Dockery, D. W.: Health effects of fine particulate air pollution: Lines that connect, J. Air Waste Manage. Assoc., 56, 709–742, 2006.

Poulain, L., Spindler, G., Birmili, W., Plass-Dulmer, C., Wiedensohler, A., and Herrmann, H.: Seasonal and diurnal variations of particulate nitrate and organic matter at the IfT research station Melpitz, Atmos. Chem. Phys., 11, 12579–12599, doi:10.5194/acp-11-12579-2011, 2011.

Saarikoski, S., Carbone, S., Decesari, S., Giulianelli, L., Angelini, F., Canagaratna, M., Ng, N. L., Trimborn, A., Facchini, M. C., Fuzzi, S., Hillamo, R., and Worsnop, D.: Chemical characteri-

zation of springtime submicrometer aerosol in Po Valley, Italy, Atmos. Chem. Phys., 12, 8401–8421, doi:10.5194/acp-12-8401-2012, 2012.

Slowik, J. G., Vlasenko, A., McGuire, M., Evans, G. J., and Abbatt, J. P. D.: Simultaneous factor analysis of organic particle and gas mass spectra: AMS and PTR-MS measurements at an urban site, Atmos. Chem. Phys., 10, 1969–1988, doi:10.5194/acp-10-1969-2010, 2010.

Spracklen, D. V., Jimenez, J. L., Carslaw, K. S., Worsnop, D. R., Evans, M. J., Mann, G. W., Zhang, Q., Canagaratna, M. R., Allan, J., Coe, H., McFiggans, G., Rap, A., and Forster, P.: Aerosol mass spectrometer constraint on the global secondary organic aerosol budget, Atmos. Chem. Phys., 11, 12109–12136, doi:10.5194/acp-11-12109-2011, 2011.

Sun, Y. L., Zhang, Q., Schwab, J. J., Demerjian, K. L., Chen, W. N., Bae, M. S., Hung, H. M., Hogrefe, O., Frank, B., Rattigan, O. V., and Lin, Y. C.: Characterization of the sources and processes of organic and inorganic aerosols in New York city with a high-resolution time-of-flight aerosol mass spectrometer, Atmos. Chem. Phys., 11, 1581–1602, doi:10.5194/acp-11-1581-2011, 2011.

Ulbrich, I. M., Canagaratna, M. R., Zhang, Q., Worsnop, D. R., and Jimenez, J. L.: Interpretation of organic components from positive matrix factorization of aerosol mass spectrometric data, Atmos. Chem. Phys., 9, 2891–2918, doi:10.5194/acp-9-2891-2009, 2009.

Zhang, Q., Jimenez, J. L., Canagaratna, M. R., Allan, J. D., Coe, H., Ulbrich, I., Alfarra, M. R., Takami, A., Middlebrook, A. M., Sun, Y. L., Dzepina, K., Dunlea, E., Docherty, K., DeCarlo, P. F., Salcedo, D., Onasch, T., Jayne, J. T., Miyoshi, T., Shimono, A., Hatakeyama, S., Takegawa, N., Kondo, Y., Schneider, J., Drewnick, F., Borrmann, S., Weimer, S., Demerjian, K., Williams, P., Bower, K., Bahreini, R., Cottrell, L., Griffin, R. J., Rautiainen, J., Sun, J. Y., Zhang, Y. M., and Worsnop, D. R.: Ubiquity and dominance of oxygenated species in organic aerosols in anthropogenically-influenced Northern Hemisphere midlatitudes, Geophys. Res. Lett., 34, L13801, doi:10.1029/2007GL029979, 2007.

Zhang, Q., Jimenez, J., Canagaratna, M., Ulbrich, I., Ng, N., Worsnop, D., and Sun, Y.: Understanding atmospheric organic aerosols via factor analysis of aerosol mass spectrometry: a review, Anal. Bioanal. Chem., 401, 3045–3067, 2011.